German Journal of Veterinary Research
eISSN:2703-1322

Research article

In vitro matured bovine oocytes in the presence of vascular endothelial growth factor–D: A Raman spectroscopy analysis

Luis E. Jimenez[1,2], Mariela Roldán-Olarte[3,4*], Alfredo N. Dominguez[1,5] and Rosa M. S. Álvarez[1,2*]

[1] Instituto de Química del Noroeste Argentino (INQUINOA), CONICET-UNT, Tucumán, Argentina
[2] Instituto de Química Física, Facultad de Bioquímica, Química y Farmacia, UNT, San Lorenzo 456, Tucumán T4000CAN, Argentina
[3] Instituto Superior de Investigaciones Biológicas (INSIBIO), CONICET-UNT, Tucumán, Argentina
[4] Instituto de Biología, Facultad de Bioquímica, Química y Farmacia, UNT, Chacabuco 461, Tucumán T4000ILI, Argentina.
[5] Instituto de Química Orgánica, Facultad de Bioquímica, Química y Farmacia, UNT, Ayacucho 471, Tucumán T4000INI, Argentina

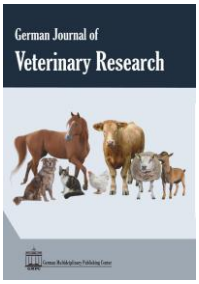

Article History:
Received: 4-Oct-2024
Accepted: 4-Jan-2025

***Corresponding author:**
Mariela Roldán-Olarte
eugenia.roldanolarte@fbqf.unt.edu.ar
Rosa M. S. Álvarez
maria.alvarez@fbqf.unt.edu.ar

Abstract

Raman microscopy is a powerful tool for examining mammalian female gametes and identifying molecular markers to evaluate their competence after *in vitro* maturation (IVM). However, its application to comprehensively analyze the biochemical changes induced in oocytes by vascular endothelial growth factor D (VEGF–D) enrichment during IVM remains largely unexplored, although various media supplements are commonly used to optimize IVM protocols. This study presents the first application of Raman spectroscopy to investigate the effect of VEGF–D supplementation on the biochemical composition of *in vitro* matured bovine oocytes. Spectral profiles of zona pellucida-free oocytes matured for 18 and 22 hours in standard and VEGF–D–enriched media were compared. The differences in specific marker bands were correlated with the attained maturational status. Multivariate statistical analysis supported the spectral interpretations, revealing an increased overall content of proteins, lipids, and carbohydrates in the cytoplasm of oocytes matured in the presence of VEGF–D. This sensitive methodology shows promise for improving culture conditions and enhancing *in vitro* maturation rates in future research.

Keywords: Cytoplasmatic maturation; ZP–free Oocytes; Multivariate analysis; Raman microscopy; Supplemented medium; Growth factors

Citation: Jimenez, L. E., Roldán-Olarte, M., Dominguez, A. N., and Álvarez, R. M. S. 2025. In vitro matured bovine oocytes in the presence of vascular endothelial growth factor–D: A Raman spectroscopy analysis. Ger. J. Vet. Res. 5 (1): 62–75. https://doi.org/10.51585/gjvr.2025.1.0120

Introduction

During the last decade, Raman microscopy has established itself as a reliable technique for evaluating the maturation state of oocytes in various mammalian species and identifying molecular markers that facilitate the investigation of their competence after undergoing different maturation procedures (Wood et al., 2008; Bogliolo et al., 2020; Davidson et al., 2013; Ishigaki et al., 2019; Rizo et al., 2016; Jimenez et al., 2019, 2022). Thanks to the sensitivity of this technique, it is possible to determine the global molecular composition of the cell and monitor biochemical and structural modifications. For instance, Bogliolo et al. (2012) detected alterations in the secondary structure of zona pellucida (ZP) glycoproteins in vitrified sheep oocytes, while Rusciano et al. (2017) reported changes in protein folding in both the ZP and cytoplasm, as well as a decrease in cytoplasmic unsaturated lipid content in bovine oocytes subjected to vitrification/devitrification. Our group has also studied the biochemical and structural changes in bovine oocytes, focusing separately on the ZP and cytoplasm during the *in*

vitro maturation (IVM) process (Rizo et al., 2016; Jimenez et al., 2019, 2022). Key findings included ZP glycoprotein reorganization and the evolution of cytoplasmic protein, lipid, and carbohydrate content, revealing that approximately 80% of oocytes reached the MII stage. Recognizing the limitations of IVM in terms of both the rate and quality of matured oocytes (Lonergan and Fair, 2016; Rizos et al., 2002), numerous modifications to IVM protocols have been proposed (Ayman et al., 2016). Previous studies have explored various growth factor supplements to address these constraints. For instance, Anchordoquy et al. (2015) demonstrated that VEGF165 significantly increased blastocyst rates in bovine oocytes. Further studies suggested that the related growth factor VEGF–D may offer similar benefits, as it has been shown to increase nuclear maturation percentages and enhance the expression of specific genes in cumulus cells (unpublished results).

In this context, this study aims to characterize the biochemical profile of *in vitro* matured bovine oocytes following VEGF–D supplementation, building upon our established methodology to monitor the evolution of the major cytoplasmic bio-components. We focus on the last four hours of maturation, which is crucial for oocyte maturity (Jimenez et al., 2022). By comparing spectral profiles of oocytes subjected to IVM for 18 and 22 hours, with and without VEGF–D supplementation, we validate the suitability of our Raman-based method for studying this complex biochemical system in different conditions.

Material and methods

Ethical approval

The experiments described did not require ethical approval from the Ethics and Animal Welfare Committee of the National University of Tucumán (Comité Institucional para el Cuidado y Uso de Animales de Laboratorio de la UNT (CICUAL-UNT) Resolución 0259/2015). Only bovine ovaries obtained as a byproduct from a local abattoir collected post-mortem from slaughtered heifers were used; no procedures were performed on living animals.

Cumulus oocytes complexes collection

Bovine ovaries were collected from slaughtered heifers (*Bos taurus*) at a local abattoir. After transportation to the laboratory at 25–30°C, they were washed three times with warm sodium phosphate buffer (PBS; pH 7.4). Cumulus–oocyte complexes (COCs) were obtained by aspirating ovarian follicles (2–8 mm in diameter) using an 18-G needle connected to a 5 mL disposable syringe containing ~1mL of Tirodes Albumin Lactate Pyruvate Medium (TALP) supplemented with 10 mM N-2-hydroxyethylpiperazine-N'-2-ethane-sulfonic acid (HEPES, Genbiotech, Argentina) and 10%(v/v) fetal bovine serum (FBS, Natocor, Argentina). Immature COCs (n=80) were meticulously selected based on morphological criteria using a stereoscopic microscope (Olympus SZ51). Only oocytes with a homogeneous cytoplasm, surrounded by at least three compact layers of cumulus cells, were chosen (see Figure 1A). Following two washes in TALP–HEPES medium, COCs were subsequently processed to obtain *in vitro* matured COCs.

***In vitro* maturation**

IVM of bovine COCs was performed following the protocol established by García et al. (2015a). Immature COCs were randomly assigned to four groups, 20 COCs of each, for *in vitro* maturation. Each group was then subdivided into two sub-groups of 10 COCs, resulting in eight sub-groups cultured in separate 100 µL droplets of the respective media. Four droplets contained a standard *in vitro* maturation medium, consisting of tissue culture medium –199 (TCM–199, Gibco, USA) supplemented with 10% FBS, 0.375 IU mL^{-1} human follicular stimulating hormone plus luteal hormone (HMG Ferring, Argentina), 0.13 mmol L^{-1} sodium pyruvate (Sigma P4562, USA), and 1% antibiotic-antimycotic solution (Gibco product 15240, USA). The remaining four droplets contained a medium supplemented with 100 ng mL^{-1} VEGF–D, comprising 90 µL of standard medium and 10 µL of VEGF–D solution (Sigma-Aldrich, product V6012, Argentina).

All culture droplets were covered with mineral oil (Fisher Scientific, USA) and maintained under IVM conditions (38.5°C with 5% CO_2 in an air atmosphere) (see Figure 1B). In each maturation medium, two sub-groups were cultured for 18 hours, while the other two were cultured for 22 hours, the duration required to complete the maturation process (García et al., 2015b). This approach ensured that each maturation process was duplicated, maintaining consistency across the experiments.

Preparation of oocytes for Raman analyses

Cumulus cells (see Figure 1C) from all treated COC groups were removed by pipetting into a warm TALP–HEPES medium containing 0.3 mg mL^{-1} hyaluronidase (Sigma Aldrich, USA) following a previously described protocol (García et al., 2015a). Cumulus cell-free oocytes (Figure 1D) were washed three times with PBS containing 1% bovine serum albumin (BSA, DSF Lab, Argentina). Subsequently, oocytes were treated with 0.4% (w/v) pronase (*Streptomyces griseus* protease, Sigma, USA) to digest the ZP completely. This step was necessary to evaluate the cytoplasm without ZP interference (Jimenez et al., 2019, 2022). Only oocytes exhibiting visually homogeneous ooplasm were destined for Raman analysis (see Figure 1E). Cells partially damaged during ZP removal were rejected. The two subgroups treated under identical conditions were then combined, resulting in a final number of 12 oocytes selected per group, with four groups generated in this study. All the selected ZP–free oocytes were fixed for 30 minutes in a 4% (w/v) paraformaldehyde solution (Rusciano et al., 2017), washed three times in PBS/BSA, and stored at 4°C for later evaluations.

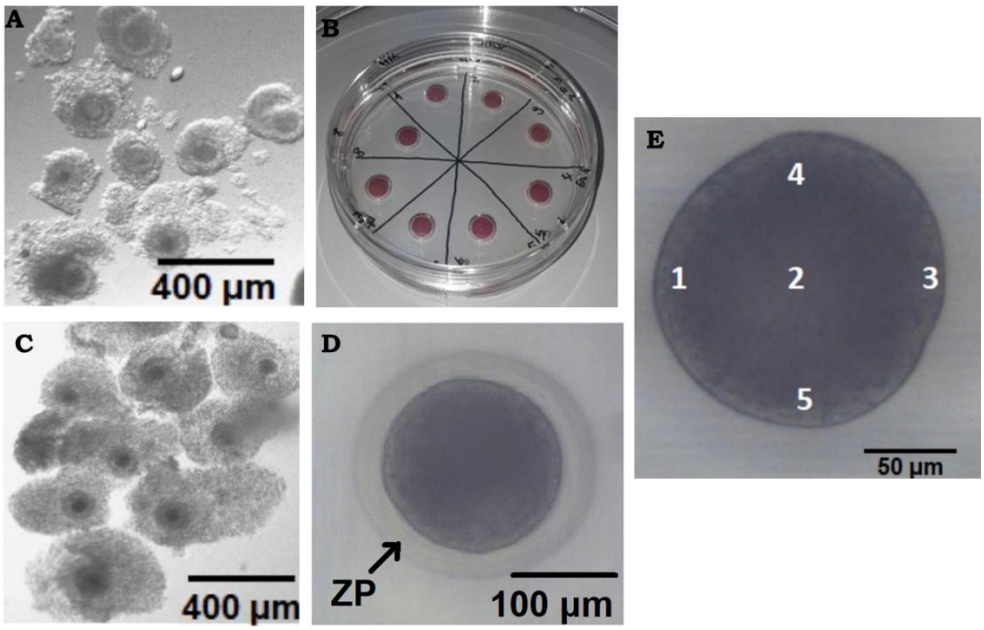

Figure 1: Images of bovine oocytes. A) immature COCs; B) *in vitro* maturation by drop culture; C) COCs matured *in vitro* for 22 hours; D) Cumulus cell-free oocyte, showing the intact ZP; E) ZP-free oocyte matured *in vitro* for 22 hours. The numbers in E) indicate approximate points from where Raman spectra of the cytoplasm were recorded. The photographs A) and C) were captured using a stereoscopic microscope, while a confocal Raman microscope with a 20× objective was used for D) and E).

Raman microscopy measurements

Raman measurements were obtained from the cytoplasm of each of the 48 selected ZP-free oocytes, individually transferred to a gold-coated slide in 5 µL of PBS. Spectra ranging between 3500 and 50 cm^{-1} were collected with a DXR confocal Raman microscope (Thermo Fisher Scientific, USA). The microscope, with a spectral resolution of 5 cm^{-1}, was equipped with a motorized stage providing a spatial resolution of 3 µm (x and y axes) and a confocal depth resolution of 2 µm (z-axis). A solid-state laser with a 780 nm diode pump was used for excitation (24 mW power), and a 50 µm slit confocal aperture was employed for data collection. The samples were focused on using a 20× objective. To prevent oocyte dehydration caused by prolonged irradiation, excess PBS (5 µL) was used during the measurements, and a maximum of five sampling points per oocyte were set (Jimenez et al., 2019, 2022). This ensured that the samples remained in good condition throughout the spectral collection. The sampling points in the cytoplasm covered both peripheral and central regions of the outermost layers of each oocyte (see Figure 1E).

Individual spectra were acquired from each sampling point by accumulating 40 exposures of 3 seconds each. A total of 240 individual spectra of cytoplasm were collected for this study. Additionally, the Raman spectrum of the PBS medium was recorded under the same conditions

as the cytoplasm. All spectroscopic experiments were carried out at room temperature.

Data analysis and statistics

The OMNIC-8 software (Thermo Scientific, USA) was used to process the 3100–900 cm^{-1} spectral data (Jimenez et al., 2019, 2022). The PBS spectrum was subtracted from each cytoplasm spectrum. The observed flattening of the spectral profile in the region of 3300–3050 cm^{-1}, along with the reduction of the band at 1616 cm^{-1}, indicated the effective elimination of the PBS spectral contribution (Rizo et al., 2016). Subsequently, all spectra underwent individual baseline correction using the linear algorithm provided by the OMNIC–8 software and were smoothed with 13 data points using the Savitzky-Golay algorithm (Savitzky and Golay, 1964).

The main biocomponents of the cytoplasm exhibit a non-uniform distribution, leading to slight spectral variations among the individual spectra of each oocyte. The arithmetic mean of the five spectra collected from each cell was calculated, resulting in a single average spectrum for each oocyte. Consequently, the total number of average spectra obtained in this study was 48 (twelve average spectra per group across four groups of oocytes with different treatments). In addition, this averaging procedure reduces noise and increases the signal-to-noise ratio in the resulting spectra. Since no significant differences were observed among the twelve average spectra from oocytes within a given group, a representative spectrum was generated for each group using all corresponding average spectra. Thus, four representative spectra were created in this study: two corresponding to oocytes subjected to IVM in the standard medium and separately cultured for 18 and 22 hours, and two corresponding to oocytes developed in medium supplemented with the VEGF–D factor, also separately treated for 18 and 22 hours. The representative spectra were labeled as Cyt–18h–C, Cyt–22h–C, Cyt–18h–F, and Cyt–22h–F, with "C" representing "control" and "F" representing "factor." To better visualize the differences between two representative spectra, arithmetic subtraction was performed. The spectrum in the standard medium was subtracted from the spectrum in the supplemented medium, with the subtraction factor automatically determined for the entire spectral region of 3100–900 cm^{-1} (Sosa Morales and Alvarez, 2016).

To provide valuable insights into protein secondary structure, the spectral region between approximately 1700 and 1600 cm^{-1}, associated with the amide I (AmI) vibration of proteins, was subjected to peak fitting and deconvolution using the GRAMS/32 software (Thermo Scientific, USA). Initially, the number of contributing band components and their positions were determined by calculating the second derivative of the representative spectrum. This procedure helps reveal peaks barely observed as shoulders in the original spectrum and find the exact location (center) of those shoulders. Based on the Levenberg-Marquardt method, the best-fitting approach was applied using Voigt functions (Marquardt, 1963) to optimize each component's position, height, Gaussian width, and Lorentzian width. The four parameters were set free while the number of peaks underlying the original curve was fixed, and iterations were allowed until the solution converged. The best fit was visually evaluated by superimposing the reconstituted curve on the original spectrum (Rizo et al., 2016; Jimenez et al., 2019, 2022).

Statistical analysis was performed using the INFOSTAT-2013 software (FCA-UNC, Argentina). The 48 average spectra were analyzed among the four mentioned groups. Spectral preprocessing and averaging were performed as described above. Student's t-tests were conducted ($p<0.01$) to compare mean intensities of characteristic peaks related to carbohydrates (approximately at 1040 cm^{-1}, νC-O/δCOH), proteins (approximately at 1340 and 1002 cm^{-1}, δCCαH and δ_sPhe, respectively), and lipids (approximately at 1300 and 1062 cm^{-1}, τCH_2 and $\nu_{as}(C\text{-}C)_T$, respectively). These peaks were extracted from the second derivative of all the average spectra within each group (n=12 per group) using the OMNIC-8 software. The second derivative enhances subtle spectral differences, improving the sensitivity of the analysis (Davidson et al., 2013; Bogliolo et al., 2012). A two-way analysis of variance (ANOVA) was performed to assess the effects of culture medium (standard vs. VEGF–D supplemented) and maturation time (18h vs. 22h) and their interactions on the mean intensities of the same marker bands. This analysis was followed by a post-hoc Tukey test to determine which specific group means differed significantly ($p<0.05$). Additionally, it was determined whether the size of

each group (n=12) was adequate through a power analysis using ANOVA. The power was calculated from the values of η^2_p with a 95% confidence interval and the corresponding Cohen's f. A desired power level of 0.80 was established. The observed power was calculated based on the sample size and the estimated effect size derived from the data.

Principal component analysis (PCA) was then performed on the same marker peaks extracted from the second derivative spectra. PCA identified the main trends within the spectral data by creating a small set of base variables (the principal components, PC) that condense information while minimizing loss. Scores and loadings plots were generated to visualize sample clustering and interpret the primary sources of spectral variation (Jimenez et al., 2019, 2022; Bogliolo et al., 2013).

Results and discussion

Raman spectroscopy analysis

To evaluate the effect of culturing in a medium supplemented with VEGF–D on the biochemical profile of bovine oocyte cytoplasm, representative Raman spectra from oocytes matured *in vitro* for 18 and 22 hours in the presence of VEGF–D (Cyt-18h-F and Cyt-22h-F, respectively) were compared with spectra from oocytes matured *in vitro* in a standard medium (Cyt-18h-C and Cyt-22h-C). Figure 2 shows the truncated regions 3100-2800 cm^{-1} and 1800-900 cm^{-1} of the four groups' representative spectra. Differences in the relative intensities and contours of specific bands were considered indicators of alterations induced by the growth factor in the relative abundances of the main bio-components.

The identification and assignment of Raman bands corresponding to specific vibrations of proteins, lipids, and carbohydrates that dominate the spectral profile of the cytoplasm have been reported for bovine oocytes and other mammalian species (Davidson et al., 2013; Jimenez et al., 2019, 2022; Bogliolo et al., 2013). The spectral region between 3100 and 2800 cm^{-1} is characterized by containing the most intense bands of the spectrum, which correspond to the C-H stretching of all the biomolecules present in the cytoplasm: the symmetric stretching of methyl groups (ν_sCH_3 at 2930 cm^{-1}) and the anti-symmetric and symmetric stretching of methylene groups ($\nu_{as}CH_2$ at 2888 cm^{-1} and ν_sCH_2 at 2851 cm^{-1}, respectively). The spectral region known as the "fingerprint zone" (between 1800 and 900 cm^{-1}) stands out due to numerous bands specific to different bio-components. These signals have been extensively analyzed in mammalian oocytes. Among these, the most intense band observed in this region across all representative spectra corresponds to the symmetric deformation mode of the methylene and methyl groups ($\delta CH_2/CH_3$), with a maximum at approximately 1440 cm^{-1}. Since all cytoplasmic macromolecules contribute to this signal, it serves as a reference for determining the relative intensities of specific bands associated with each bio-component. Below 900 cm^{-1}, the cytoplasm spectrum is characterized by a low signal-to-noise ratio that compromises its analysis; therefore, bands in this region are often excluded from spectral studies in mammalian oocytes (Wood et al., 2008; Davidson et al., 2013; Bogliolo et al., 2013). Table 1 includes the proposed assignments for most bands identified in the specified spectral regions. The effect produced by VEGF–D in the oocyte's cytoplasm during the IVM was evaluated by comparing the representative spectra of cells cultivated for the same period in the presence and absence of the growth factor.

Cyt-18h-C Vs Cyt-18h-F

In the C-H stretching region, the Cyt-18h-F spectrum showed the ν_sCH_3 band (2931 cm^{-1}) more intense than Cyt-18h-C, while the bands at 2881 cm^{-1} ($\nu_{as}CH_2$) and at 2852 cm^{-1} (ν_sCH_2) did not experience significant changes. It has been proposed that the Raman intensities ratio between the peaks corresponding to ν_sCH_3 and ν_sCH_2 (I_{2931}/I_{2881}) is a parameter that allows estimating variations in the relative content of proteins and lipids since the methyl band is mainly attributed to proteins and the methylene signals receive primarily contributions from lipids (Czamara et al., 2017; Krafft et al., 2005). The I_{2931}/I_{2881} ratio was calculated to be approximately 15% higher in the Cyt-18h-F spectrum than in the control, suggesting an increase in protein content upon 18 hours of culture *in vitro* in the presence of VEGF–D.

In the spectral region between 1800 and 900 cm^{-1}, additional differences confirming the increase in protein content in Cyt-18h-F were observed: I) the enhancement of the sharp bands at 1617, 1589, 1206, and 1002 cm^{-1}, which are

characteristic of aromatic amino acids; II) a marked intensification of the band at 1340 cm^{-1}, assigned to the deformation of the protein backbone with α-helix conformation (δC-$C_α$-H), where the I_{1340}/I_{1440} intensity ratio showed an increase of approximately 50% with respect to the control spectrum; III) in line with this observation, the band contour at approximately 1250 cm^{-1}, attributed to an overlap between the amide III (AmIII) mode of proteins and the C=CH deformation mode of unsaturated lipids, changed visibly; the sharp feature centered at 1267 cm^{-1} in the Cyt-18h-C spectrum was interpreted as a dominant contribution from lipids, while in Cyt-18h-F, the broader shape of the band suggests that the protein AmIII components gained intensity; and IV) the intense band with a maximum at 1655 cm^{-1} showed a more irregular contour in Cyt-18h-F, indicating a more significant contribution from the different components of the AmI mode (Jimenez et al., 2022; Rygula et al., 2013; Wu et al., 2011). The complexity of this specific spectral region, where the AmI modes of proteins and N-acetylated carbohydrates overlap with the C=C stretching of unsaturated lipids, necessitated a more detailed study. The upper panel of Figure 3 presents the two compared spectra overlaying, which better visualizes spectral differences with the C=C stretching of unsaturated lipids, necessitating a more detailed study, as will be discussed below. In general, carbohydrate bands are challenging to observe in the spectra of cytoplasm due to their low intensity and overlapping with stronger bands from proteins and lipids. However, when comparing the Cyt-18h-F and Cyt-18h-C Raman spectra, subtle differences in carbohydrate features were observed, such as enhancements and more precise definitions. Specifically, the following bands were notable: the symmetric stretching of the carboxylate group ($ν_sCOO^-$) at approximately 1405 cm^{-1}, the deformation of the methyl group ($δCH_3$) at 1375 cm^{-1}, and a shoulder peak assigned to coupled vibrations between the stretching and deformation of the C-O bond (νC-O/δCOH) at 1040 cm^{-1} (as shown in Figure 2).

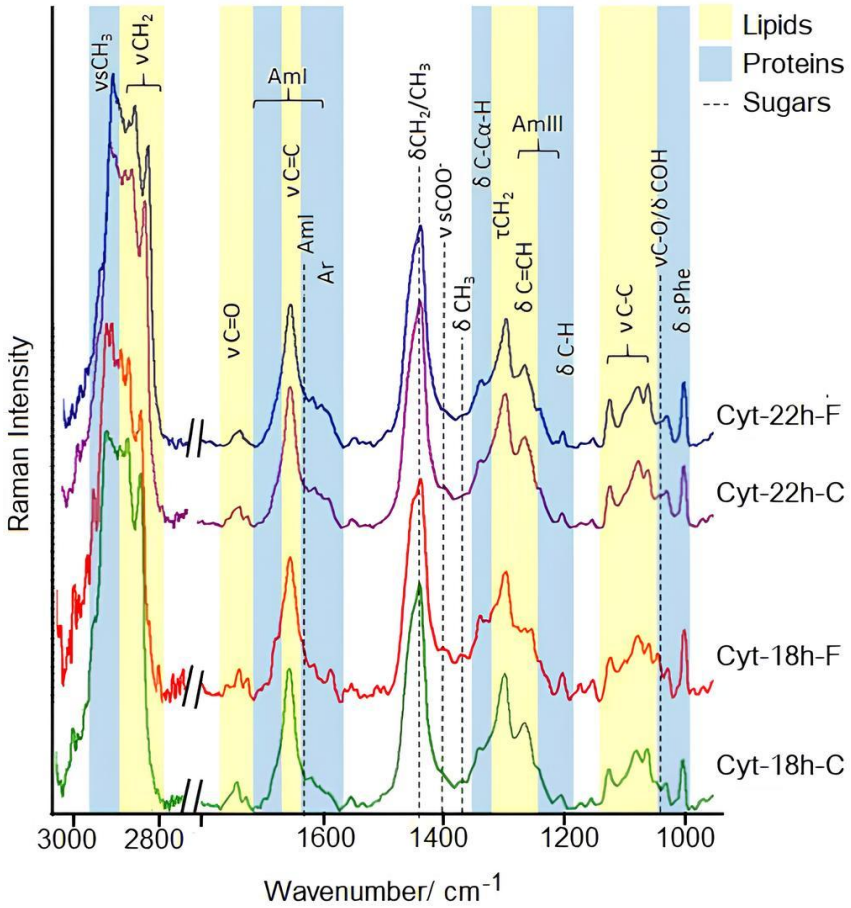

Figure 2: Representative Raman spectra of the cytoplasm of oocytes matured *in vitro* for 18 and 22 hours in standard medium and medium supplemented with VEGF–D. The spectra, truncated in the regions 3000-2800 cm^{-1} and 1800-900 cm^{-1}, are normalized with the band at 1440 cm^{-1} ($δCH_2/CH_3$). Light blue areas indicate protein vibrations, while yellow areas correspond to lipid bands. Carbohydrate bands were marked with dotted lines.

Table 1: Wavenumbers (cm^{-1}), relative intensities, and tentative assignments of the bands observed in the regions 3100-2800 cm^{-1} and 1800-900 cm^{-1} of the representative spectra of the four groups generated in this study.

Cyt-18h-C	Cyt-18h-F	Cyt-22h-C	Cyt-22h-F	Tentative assignment
2930vs	2932vs	2934vs	2934vs	$\nu_s CH_3$ (Proteins, Lipids)
2882vs	2888vs	2884vs	2883vs	$\nu_{as} CH_2$ (Proteins, Lipids)
2852vs	2853vs	2853vs	2851vs	$\nu_s CH_2$ (Lipids)
1743w	1741w	1742w	1742w	νC=O (Phospholipids)
1729w	1727w	1729w	-	νC=O (Triglycerides)
1657s	1657s/wd	1656s/wd	1657s/wd	AmI (Proteins)/νC=C (Lipids)
1620m	1617m	1619m	1617m	νTyr
1606sh	1605w	1606sh	1606sh	νPhe
1586sh	1589w	1590sh	1592sh	νPhe
1440vs	1440vs	1440vs	1440vs	$\delta CH_2/CH_3$
1405sh	1404m	1406sh	1406sh	$\nu_s COO^-$ (Sugar)
1340m	1341s	1341s	1340s	$\delta CC_\alpha H$ (Proteins)
1300s	1300s	1299s	1299s	τCH_2 (Lipids)
1267m	1267m	1268s	1268s	AmIII (Proteins)/δC=CH (Lipids)
~1258sh	~1258sh	~1260sh	~1260m	AmIII (Proteins)
1206w	1206w	1206w	1205w	δPhe
1127m	1126m	1127m	1127m	$\nu_s(C\text{-}C)_T$ (Lipids)
1100sh	1101w	1100sh	1100sh	νC-O/δCOH (Sugar)// $\nu_s PO^-_4$
1082m	1079m	1080m	1080m	$\nu(C\text{-}C)_G$ (Lipids)
1063m	1062m	1063w	1062w	$\nu_{as}(C\text{-}C)_T$ (Lipids)
1040w	1040w	1040sh	1039sh	ν C-O/δCOH (Sugars)
~1033w	1032w	1033w/wd	1033w	νC-C (Proteins)
1002w	1002m	1001m	1002m	δ_sPhe

vs: very strong, s: strong, m: medium, w: weak, wd: wide band, sh: shoulder, ν: stretching, δ: deformation, τ: twist. The bands that exhibited differences when comparing the representative spectra of groups grown for the same period are highlighted.

In contrast, most lipid vibration bands did not show differences between the two spectra, which could suggest significant changes in the lipid content. The exception worth mentioning was the 1080 cm^{-1} signal assigned to the C-C stretching of methylenes in *gauche* conformation ($\nu(C\text{-}C)_G$) within the acyl chains of lipids. This signal is typically associated with the phase state of the lipids. It has been proposed that the intensity ratio between this band and the one assigned to the C-C stretching of methylenes in trans conformation ($\nu(C\text{-}C)_T$ at 1062 cm^{-1}) reveals the relative population of *gauche* conformers within the hydrocarbon chains. A higher proportion of *gauche* versus trans conformations indicates greater membrane fluidity (Krafft et al., 2005; Okotrub et al., 2018). In this case, the I_{1080}/I_{1062} ratio was approximately 13% higher in the Cyt-18h-F spectrum than in the control, suggesting that greater fluidity of the lipid membranes was manifested in the oocytes treated with VEGF–D. This interpretation aligns with a previous study that found a higher unsaturated fatty acid content in oocytes at the MII stage than at the GV stage (Wood et al., 2008).

Spectral differences are better visualized by overlying the two compared spectra, as presented in the upper panel of Figure 3. The difference spectrum obtained by spectral subtraction of Cyt-18h-C from Cyt-18h-F is also included. Figure 4 shows the decomposition and fitting of the complex spectral region comprised between 1700 and 1600 cm^{-1} for the four representative spectra. Based on the extensive literature on the protein AmI band, the components at approximately 1683, 1672, 1663, and 1651 cm^{-1} were assigned to the turns, β-sheets, random coils, and α-helices conformations, respectively. Additionally, the more substantial component centered around 1656 cm^{-1} was attributed to the C=C stretching (νC=C) of unsaturated lipids, while that at about 1635 cm^{-1} corresponded to the AmI mode of N-acetylated carbohydrates (Rizo et al., 2016; Jimenez et al., 2019, 2022). Specifically, the component at 1657 cm^{-1} in Cyt-18h-C (Figure 4A) demonstrated a significantly dominant contribution within this spectral region. This observation explained the narrow and uniform contour of the envelope band and aligned with our previous findings regarding the initial eighteen hours of *in vitro* culture. During this period, the primary event occurring in the cytoplasm of bovine oocytes was a marked

increase in lipid content (Jimenez et al., 2022). In contrast, the decomposition of Cyt-18h-F (Figure 4C) revealed a notable intensification of the protein AmI components, especially those corresponding to the β-sheet and α-helix domains (1671 and 1649 cm^{-1}, respectively). This finding corresponded with the enhancement of the δC-$C_α$-H band (at 1340 cm^{-1}) and the change in the shape of the AmIII band (at 1250 cm^{-1}), both mentioned earlier (items II and III). Furthermore, the AmI component of N-acetylated carbohydrates (approximately at 1635 cm^{-1}) also appeared more intense in Cyt-18h-F with respect to the control, in agreement with the behavior observed in other sugar bands.

The most significant spectral differences between the two groups cultured *in vitro* for eighteen hours are characterized by notable intensifications and enhanced definitions of several bands associated mainly with proteins and sugars in the cytoplasm of oocytes treated in the presence of VEGF–D. This highlights the potential impact of this growth factor on oocyte biochemical composition. This sets the stage for comparing the spectra of oocytes cultured for 22 hours in both media to elucidate further the effects of VEGF–D over a more extended maturation period.

Cyt-22h-C Vs Cyt-22h-F

A direct comparison between the representative spectra of the cytoplasm in oocytes matured *in vitro* for 22 hours in standard and supplemented media and the difference spectrum between them is presented in Figure 4, lower panel. At first glance, the spectral profiles appear remarkably similar to each other. However, the Cyt-22-F spectrum exhibited an I_{2931}/I_{2881} ratio approximately 12% higher than that in the control spectrum. Additionally, there was a slight enhancement of the protein bands at approximately 1617 cm^{-1} (νTyr) and 1606 cm^{-1} (νPhe), along with a widening of the band centered at 1657 cm^{-1} (AmI). All these differences suggest protein content changes caused by the culture medium's growth factor. Indeed, the spectral decomposition of the region between 1700 and 1600 cm^{-1} for both groups (Figure 4B and D) revealed a significant distinction in the contributions from the β-sheet and random coil protein domains (1672 and 1662 cm^{-1}, respectively). The component associated with the AmI mode of N-acetylated carbohydrates also appeared notably enhanced in the Cyt-22h-F spectrum.

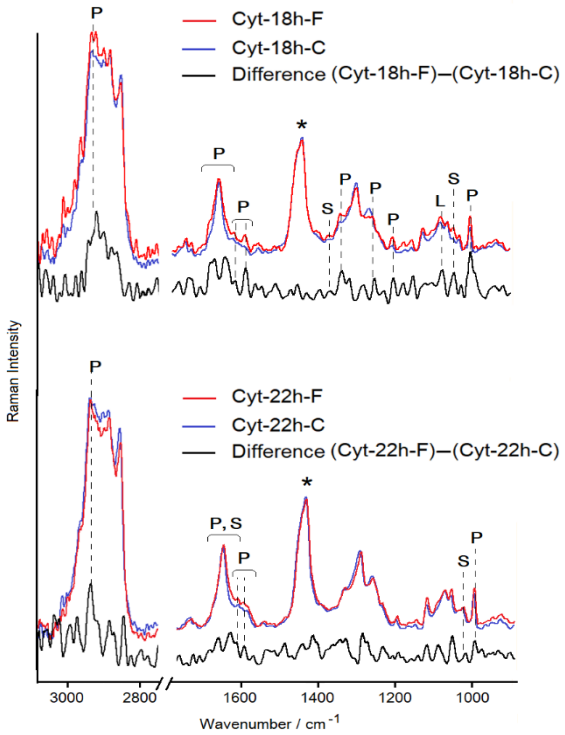

Figure 3: Main observed differences between the representative spectra, showing the comparison and difference spectra of groups culture *in vitro* for 18 (upper panel) and 22 hours (lower panel). Spectra are normalized to the band at 1440 cm^{-1}, denoted by an asterisk (*). P: protein band; L: lipid band; S: sugar band. See Figure 2 for the band assignment.

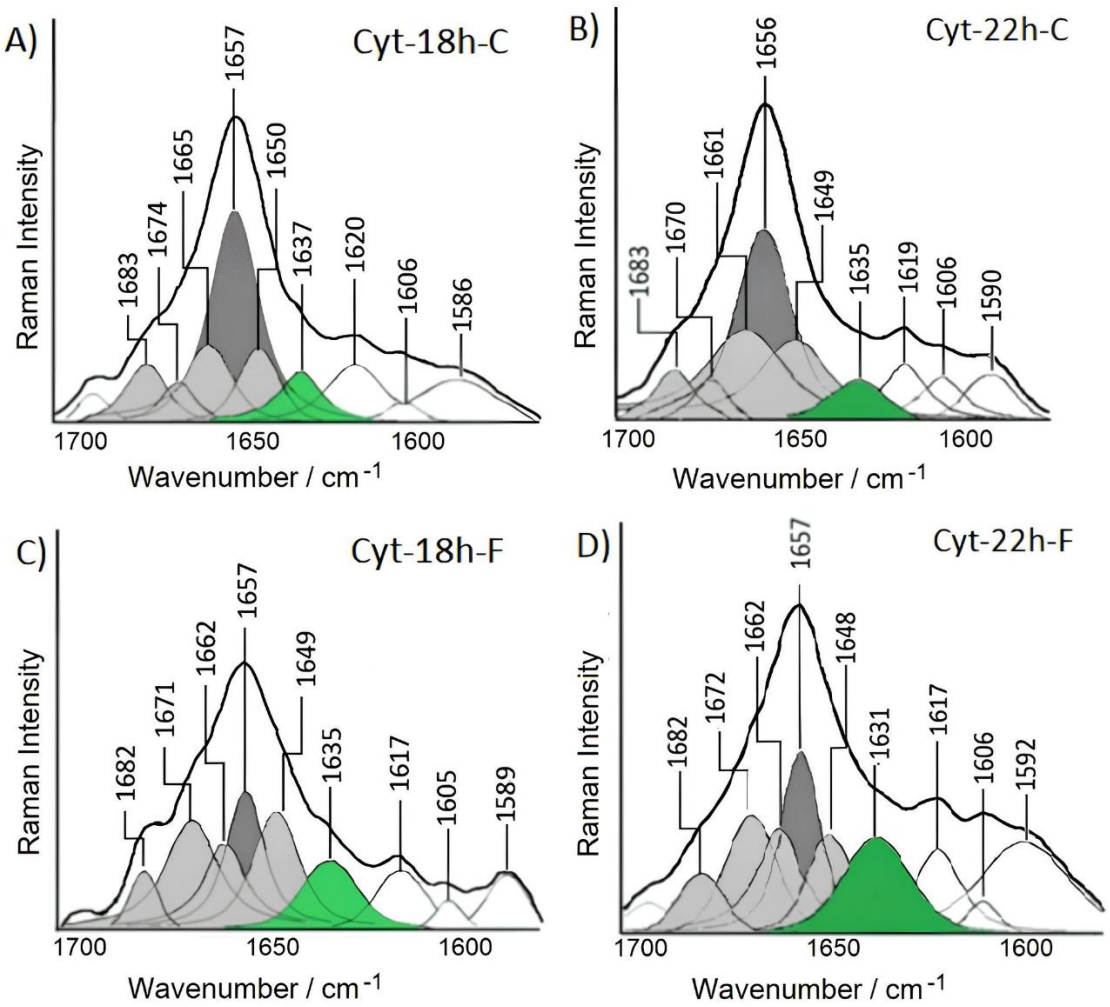

Figure 4: Spectral decomposition of the region between 1700 and 1600 cm^{-1}. Deconvolution and peak fitting procedures were applied to the representative spectra of the cytoplasm of oocytes subjected to the *in vitro* maturation process for 18 and 22 hours in standard maturation media (A and B, respectively) and media enriched with VEGF–D (C and D, respectively). Components in dark gray: νC=C of unsaturated lipids; components in light gray: protein AmI; component in green: AmI from carbohydrates.

This observation is accompanied by subtle changes in the spectral profile in regions where the contribution from the vibrational modes $\nu_s COO^-$ (around 1405 cm^{-1}) and νC-O/δCOH (at 1040 cm^{-1}), both specific to sugars, are expected (Jimenez et al., 2019, 2022; Giorgini et al., 2014; Rizo et al., 2016). The ratios I_{1405}/I_{1440} and I_{1040}/I_{1440} were approximately 20% and 50% higher, respectively, compared to the control (treatment in standard medium).

Furthermore, the weakening of both the band at 1729 cm^{-1} (assigned to the stretching of the carbonyl group of triglycerides) and the band at 1080 cm^{-1} $(\nu(C\text{-}C)_G)$ of lipids was detected in the Cyt-22h-F spectrum (Okotrub et al., 2018). All these observations suggest that VEGF–D affects the cytoplasm's overall biochemical content throughout the maturation process's final stage. Specifically, the spectral evidence indicates that incorporating VEGF–D into the culture medium increases protein content considerably shorter than required under standard conditions (Jimenez et al., 2022). In addition, the cell maintains a high carbohydrate content until the end of the process, which could provide an advantage for the oocyte when facing the *in vitro* fertilization (IVF) stage. These changes, considered improvements in cytoplasmic maturation, are complemented by results from epifluorescence microscopy showing that VEGF–D in the culture medium increases percentages of nuclear maturation (unpublished results). Moreover, Anchordoquy et al. (2015) demonstrated that the supplementation of *in vitro* maturation media with VEGF165 (another member of the VEGF family) at concentrations of

300 and 500 ng/mL significantly increased the percentage of blastocysts compared to the control group, suggesting a positive impact of this growth factor on the developmental competence of bovine oocytes. This background supports the hypothesis that the observations derived from the Raman spectrum of oocytes treated with VEGF–D may be related to enhanced competence of the cell to face IVF.

One of the molecular mechanisms by which VEGF–D could be exerting these observed effects may be through interaction with specific receptors located on the plasma membrane of the oocytes and/or in the cumulus cells that accompany them during IVM, as demonstrated by Einspanier et al. (2002). This indicates that VEGF–D may act through its receptors, activating intracellular signaling pathways that promote oocyte maturation at both the nuclear and cytoplasmic levels.

Statistical analysis

The spectral differences detected from the direct comparison between the representative spectra of the four groups of oocytes generated in this study were evaluated by statistical methods. Student's t-test, two-way ANOVA, and PCA were applied to the same variables that had been previously defined as indicators of the maturation state of bovine oocyte cytoplasm (Jimenez et al., 2019, 2022). These variables consist of the intensities of the bands at 1300 and 1062 cm^{-1}, assigned to characteristic vibrations of the acyl chains of lipids; the bands at 1340 and 1003 cm^{-1}, corresponding to protein vibrations; and the band at 1040 cm^{-1}, typical of carbohydrates, all extracted from the second derivative of the average spectrum calculated for each oocyte. A total of 48 average spectra (12 per group) were utilized for statistical analysis.

The enhancement observed by the bands at 1340 and 1002 cm^{-1} in Cyt–18h-F compared to the control spectrum was confirmed by the T-test as statistically significant differences (p<0.01) in the arithmetic means derived from the protein signals between the spectra of oocytes cultured for 18 hours. However, these bands did not show significant differences between the groups of oocytes matured for 22 hours, despite the enhancement observed in other protein bands in the representative Cyt–22h–F spectrum (e.g., the bands at approximately 1617 and 1606 cm^{-1}, assigned to νTyr and νPhe, respectively, and the AmI components at 1672 and 1662 cm^{-1}, as described above). Similarly, the addition of VEGF–D to the medium caused an increase in the arithmetic means of the lipid bands, both in oocytes cultured for 18 and 22 hours. However, the changes were not statistically significant. Interestingly, the sugar band at 1040 cm^{-1} increased significantly (p<0.01) in the growth factor-treated oocyte groups (Cyt–18h–F and Cyt–22h–F) compared to the control groups. The arithmetic means of the five marker bands in the four groups of average spectra are listed in Table 2.

Table 2: Descriptive statistics showing arithmetic mean (± standard deviation) for each combination of variable and experimental condition.

Groups (n=12)	1340	1300	1062	1040	1002	*p* Value
Cyt-18h-C	0.15±0.05	0.31±0.11	0.25±0.05	0.06±0.03	0.59±0.13	1340 (p<0.01), 1002 (p<0.01)
Cyt-18h-F	0.27±0.05	0.33±0.07	0.27±0.06	0.12±0.03	0.74±0.10	
Cyt-22h-C	0.22±0.06	0.35±0.11	0.27±0.09	0.07±0.04	0.70±0.24	1040 (p<0.01)
Cyt-22h-F	0.26±0.04	0.38±0.07	0.34±0.11	0.11±0.02	0.81±0.18	

To analyze the effects of both treatment (standard vs. VEGF–D supplemented) and *in vitro* maturation time (18h vs. 22h), the arithmetic means of each variable were compared using ANOVA (Figure 5). This analysis revealed a significant increase in the intensity of the protein band at 1340 cm^{-1} due to both VEGF–D treatment (p<0.0001) and culture duration (p=0.0325), as well as a significant interaction between the two factors (p=0.0149), indicating a time-dependent effect of VEGF–D. A statistically significant enhancement (p=0.0105) was also observed in the supplemented medium for the other selected protein band at 1002 cm^{-1}. Regarding the lipid signals, the arithmetic means for the band at 1062 cm^{-1} were found to be significantly different due to treatment (p=0.0480) and culture duration (p=0.0472), but their interaction was not detected. In contrast, the band at 1300 cm^{-1} did not show significant differences in the effects exerted by either of the two factors. Finally, the intensity of the

carbohydrate band at 1040 cm^{-1} showed a significant enhancement (p<0.0001) due to VEGF–D treatment, with no significant effects observed for culture duration or the treatment-time interaction. Tukey's post-hoc test confirmed that the VEGF–D supplemented medium significantly increased the intensities of the bands at 1340, 1062, and 1040 cm^{-1} compared to the standard medium.

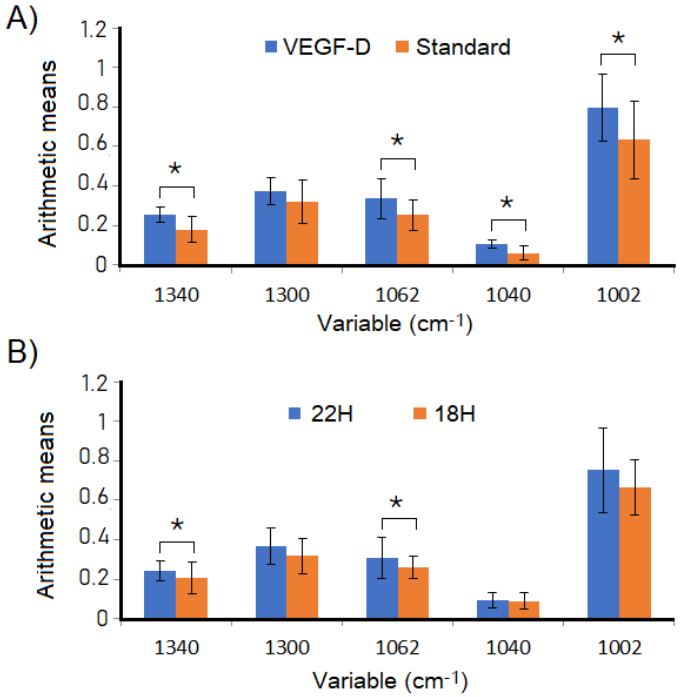

Figure 5: Arithmetic means of cytoplasmic maturation marker bands calculated using two-way ANOVA. Panel A compares the mean intensities of specific protein signals (at 1340 and 1002 cm^{-1}), lipid signals (at 1300 and 1062 cm^{-1}), and carbohydrate signals (at 1040 cm^{-1}) produced by the treatment. The standard medium is represented by orange bars, and the VEGF–D-supplemented medium is represented by blue bars. Panel B compares the effects of *in vitro* culture duration, with bars representing 18 hours (orange) and 22 hours (blue). Vertical lines represent standard deviations, and significant differences between groups are indicated by a horizontal bracket. Asterisks denote signals that present significant differences according to p<0.05, as determined by Tukey's post-hoc test.

Based on these data, the values of η^2_p were calculated with a 95% confidence interval, ranging from 0.10 to 0.45. These values correspond to medium to large effect sizes for each variable that showed significant differences. The observed power was calculated to be 0.967, 0.947, 0.471, and 0.301 for the variables at 1340, 1040, 1002, and 1062 cm^{-1}, respectively. These results indicate that the sample size used in this study (n=12 per group) is sufficient to detect significant effects with a high probability for the protein and carbohydrate variables.

The most relevant finding arising from these analyses is that VEGF–D in the culture medium accelerated protein production, as the protein content in the cytoplasm of oocytes from the Cyt-18h-F group was higher than that achieved at the end of maturation in a standard medium (Cyt-22h-C). Additionally, it was notable that the sugar content remained relatively high until the end of IVM with the supplemented medium; it has been observed that carbohydrates consistently decrease throughout the entire maturation process when a standard culture medium is used, in accordance with the well-known metabolic activity of glucose (Jimenez et al., 2019; Jimenez et al., 2022).

Additionally, PCA was performed to investigate further the relationships between the spectral data of the four groups of oocytes generated in this study. Figure 6 presents the scatterplot resulting from PCA (PC1 vs. PC2), explaining 60% of the total variance. PCA revealed that positive PC1 values were strongly correlated with spectra rich in proteins and lipids; for PC2, positive values were mainly associated with spectra exhibiting intense bands of sugars,

while negative values correlated with spectra rich in lipids. Clear distinctions were observed between the two groups of oocytes cultured for 18 hours. The control group was characterized by a dominant contribution of lipids and a relatively low sugar content, whereas the spectra of oocytes cultured in the presence of the factor clustered in the positive regions of both PC1 and PC2, indicating high proportions of proteins, lipids, and carbohydrates.

In accordance with prior studies, oocytes matured in the standard medium (Cyt-22h-C) demonstrated notable variation in scores (Jimenez et al., 2019; Jimenez et al., 2022). Most of these scores aligned with positive values of PC1 and negative values of PC2, signifying spectra rich in lipid and protein bands but with minimal sugar contributions. Conversely, certain spectra occupied an opposing region, consistent with a lower proportion of lipids and proteins (Jimenez et al., 2022). Oocytes matured in the presence of VEGF–D and exhibited high content in all three main bio-components. The overlap between most of the scores from the Cyt–18h–F and Cyt–22h–F groups confirmed the observation of the accelerating effect exerted by the factor on cytoplasmic maturation. Furthermore, this analysis suggested that the evolution of oocytes cultured in the enriched medium leads to a more homogeneous cytoplasm in terms of the main bio-components than that observed in the standard medium. The clustering of points corresponding to the Cyt–18h–F and Cyt–22h–F groups was notably tighter than that of the Cyt-22h-C group.

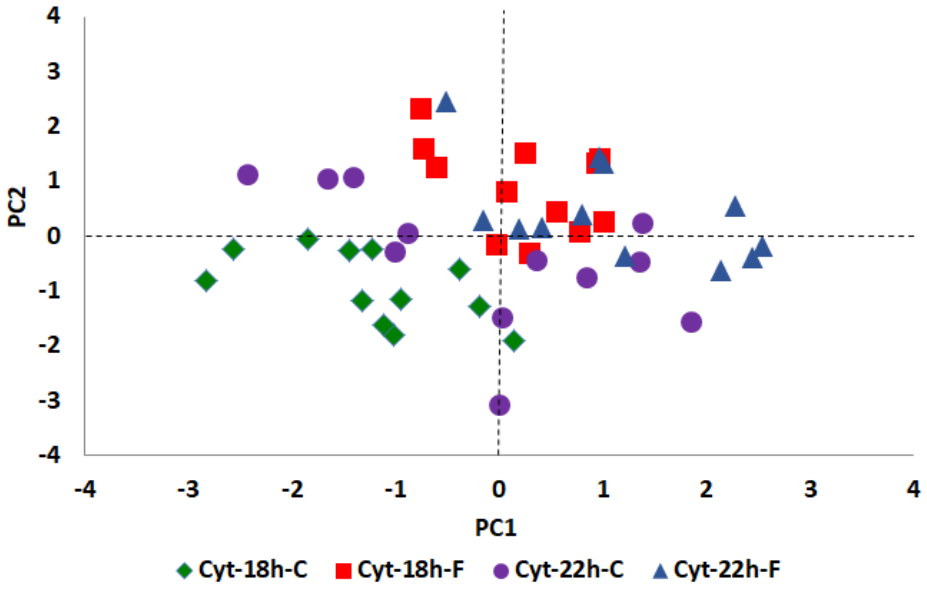

Figure 6: Principal component analysis. The components PC1 and PC2 were generated from the intensities of specific bands of proteins, lipids, and carbohydrates extracted from the second derivative spectra of the groups of *in vitro* matured oocytes for 18 and 22 hours in a standard culture medium (Cyt-18h-C, n=12 and Cyt–22h–C; n=12) and enriched with the VEGF–D factor (Cyt–18h-F, n= 12 and Cyt–22h–F; n=12).

Previous findings by Jimenez et al. (2019,2022) support the current analysis, highlighting the utility of Raman spectroscopy combined with multivariate analysis for assessing the global biochemical composition of bovine oocytes. Specifically, Jimenez et al. (2019) demonstrated significant correlations between lipid and protein content and maturation status through PCA analysis, further validated using epifluorescence microscopy. In follow-up work, Jimenez et al. (2022) confirmed the method's sensitivity in detecting lipid and protein content changes at intermediate stages of *in vitro* maturation.

While this study reaffirms the method's effectiveness in reliably identifying significant biochemical changes in oocytes induced by culture time and/or specific treatments, it is essential to acknowledge the complexities of the analytical methodology. This includes the cumbersome process of enzymatic ZP disintegration, which allows for the study of the cytoplasm without interference but ultimately renders the oocyte unusable for future experiments.

A promising alternative is to combine Raman microscopy with statistical analysis to focus on the cumulus cells. Although indirect, this strategy would enable the monitoring of oocytes

throughout the *in vitro* maturation process without causing damage, either before or during the Raman spectroscopic analysis. Furthermore, it would facilitate a more comprehensive understanding of the interactions between oocytes and cumulus cells during maturation.

Conclusions

This study represents the first approach using Raman microscopy to evaluate the effect of VEGF–D on the biochemical profile of the cytoplasm of bovine oocytes subjected to *in vitro* maturation in a medium supplemented with this growth factor. The spectral differences resulting from the comparison between oocytes treated in the supplemented medium and those cultured in the standard medium are interpreted as an increase in cytoplasmic biomolecule content, primarily proteins and carbohydrates, induced by VEGF–D. The results indicate that the incorporation of VEGF–D into the culture medium accelerates and presumably enhances the cytoplasmic maturation of bovine oocytes, which could positively impact various aspects of oocyte development and quality, favoring an increase in the percentages of blastocysts obtained *in vitro*. However, further studies are required to evaluate the response of oocytes matured in a medium supplemented with this growth factor and subsequently fertilized *in vitro* regarding cleavage and blastocyst production rates to confirm the positive impact of VEGF–D on developmental capacity.

The applied methodology, consisting of analyzing Raman spectra of ZP–free oocytes followed by multivariate statistical analysis applied to specific marker bands, has proven to be sufficiently sensitive to study the biochemical profile of oocytes treated in an enriched culture medium. This approach promises to be adequate for evaluating the effects of future modifications in the *in vitro* maturation protocol on the biochemistry of oocytes, aiming to increase maturation rates and improve the intrinsic quality of *in vitro* matured bovine oocytes.

Article Information

Funding. This work was supported by CONICET [Grant PIP2015 N°629 to R.M.S.A.] and Universidad Nacional de Tucuman, Argentina [Grants PIUNT2018 D-648-1 to M.R.O and PIUNT2018 D-604 to R.M.S.A.].

Conflicts of Interest. The authors declare no conflict of interest.

Acknowledgments. The authors would like to thank Frigorífico Calchaquí S.A. slaughterhouse, Tucumán, Argentina, for providing the biological material. A.N.D. and L.E.J. are grateful to CONICET for their Doctoral and postdoctoral fellowship, respectively. R.M.S.A. and M.R.O. are career researchers of CONICET.

Authors contribution. L.E.J.: Performed research, analyzed data, and wrote the paper; A.N.D: Analyzed data; M.R.O.: Conceived study and performed research; R.M.S.A.: Conceived study, performed research, and wrote the paper. All authors read and approved the final article.

Publisher's Note. The claims and data contained in this manuscript are solely those of the author(s) and do not represent those of the GMPC publisher, editors, or reviewers. GMPC publisher and the editors disclaim the responsibility for any injury to people or property resulting from the contents of this article.

References

Anchordoquy, J.M., Anchordoquy, J.P., Testa, J.A., Sirini, M.A. Furnus, C.C., 2015. Influence of vascular endothelial growth factor and cysteamine on *in vitro* bovine oocyte maturation and subsequent embryo development. Cell Biology International 39, 1090–1098. https://doi.org/10.1002/cbin.10481

Ayman, H., El-Aziz, A., Usama, E., Sherief, Z., Ahmed, A., 2016. Factors influencing *in vitro* production of bovine embryos: A Review. Asian Journal of Animal and Veterinary Advances 11, 737–756. https://doi.org/10.3923/ajava.2016.737.756

Bogliolo, L., Ledda, S., Innocenzi, P., Ariu, F., Bebbere, D., Rosati, I. et al., 2012. Raman microspectroscopy as a non-invasive tool to assess the vitrification-induced changes of ovine oocyte zona pellucida. Cryobiology 64, 267–272. https://doi.org/10.1016/j.cryobiol.2012.02.010

Bogliolo, L., Leoni, G.G., Ledda, S., 2020. Raman spectroscopy-based approach to study the female gamete. Theriogenology 150, 268–275. https://doi.org/10.1016/j.theriogenology.2020.01.059

Bogliolo, L., Murrone, O., Di Emidio, G., Piccinini, M., Ariu, F., Ledda, S. et al., 2013. Raman spectroscopy-based approach to detect aging-related oxidative damage in the mouse oocyte, Journal of Assisted Reproduction and Genetics, 30, 877–882. https://doi.org/10.1007/s10815-013-0046-6

Czamara, K., Majzner, K., Selmi, A., Baranska, M., Ozaki, Y., Kaczor, A., 2017. Unsaturated lipid bodies as a hallmark of inflammation studied by Raman 2D and 3D microscopy. Scientific Reports 7, 1–10. https://doi.org/10.1038/srep40889

Davidson, B., Murray, A.A., Elfick, A., Spears, N., 2013. Raman microspectroscopy can be used to investigate the developmental stage of the mouse oocyte. PLoS ONE 8, e67972–e67981 https://doi.org/10.1371/journal.pone.0067972

Einspanier, R., Schönfelder, M., Müller, K., Stojkovic, M., Kosmann, M., Wolf, E. et al., 2002. Expression of the vascular endothelial growth factor and its receptors and effects of VEGF during *in vitro* maturation of bovine cumulus-oocyte complexes (COC). Molecular Reproduction and Development 62, 29–36. https://doi.org/10.1002/mrd.10068

García, D.C., Miceli, D.C., Rizo, G., García, E.V., Valdecantos, P.A., Roldán-Olarte, M., 2015a. Expression and localization of urokinase-type plasminogen activator receptor in bovine cumulus–oocyte complexes. Zygote 24, 230–235.

https://doi.org/10.1017/S0967199415000076

Garcia, E.V., Miceli, D.C., Rizo, G., Valdecantos, P.A., Barrera, A.D., 2015b. Effect of early addition of bone morphogenetic protein 5 (BMP5) to embryo culture medium on *in vitro* development and expression of developmentally important genes in bovine preimplantation embryos. Theriogenology 5, 589–599. https://doi.org/10.1016/j.theriogenology.2015.04.018

Giorgini, E., Gioacchini, G., Sabbatini, S., Conti, C., Vaccari, L., Borini, A., Carnevali, O., Tosi, G., 2014. Vibrational characterization of female gametes: a comparative study. Analyst 139, 5049–5060. https://doi.org/10.1039/c4an00684d

Ishigaki, M., Hoshino, Y., Ozaki, Y., 2019. Phosphoric acid and phosphorylation levels are potential biomarkers indicating developmental competence of matured oocytes. Analyst 144, 1527–1534. https://doi.org/10.1039/C8AN01589ª

Jimenez, L.E., Juárez, A.C., Roldán-Olarte, M., Álvarez, M.R.S., 2022. Biochemical changes in the cytoplasm of bovine oocytes during the *in vitro* maturation process: a Raman microscopy study. Veterinary Research Communications 46, 549–562. https://doi.org/10.1007/s11259-021-09882-4

Jimenez, L.E., Roldán-Olarte, M., Álvarez, M.R.S., 2019. Raman microscopy analysis of the biochemical changes in the cytoplasm of bovine oocytes induced by an *in vitro* maturation process: interference of the zona pellucida. Chemistry Select 4, 3706–3716. https://doi.org/10.1002/slct.20180-3454

Krafft, C., Knetschke, T., Funk, R.H.W., Salzer, R., 2005. Identification of organelles and vesicles in single cells by Raman microspectroscopic mapping. Vibrational Spectroscopy 38, 85–93. https://doi.org/10.1016/j.vibspec.2005.02.008

Lonergan, P., Fair, T., 2016. Maturation of oocytes *in vitro*. Annual Review of Animal Biosciences 4, 255–268. https://doi.org/10.1146/annurev-animal-022114-110822

Marquardt, D.W., 1963. An algorithm for least-squares estimation of nonlinear parameters. Journal of the Society for Industrial and Applied Mathematics 11, 431–441. https://doi.org/10.1137/0111030

Okotrub, K.A., Mokrousova, V.I., Amstislavsky, S.Y., Surovtsev, N.V., 2018. Lipid droplet phase transition in freezing cat embryos and oocytes probed by Raman spectroscopy. Biophysical Journal 115, 1–11. https://doi.org/10.1016/j.bpj.2018.06.019

Rizo, G., Roldán-Olarte, M., Miceli, D.C., Jimenez, L.E., Álvarez, M.R.S., 2016. Structural modifications induced by an *in vitro* maturation process in zona pellucida glycoproteins. RSC Advances 6, 83429–83437. https://doi.org/10.1039/C6RA06243A

Rizos, D., Ward, F., Duffy, P., Boland, M.P., Lonergan, P., 2002. Consequences of bovine oocyte maturation, fertilization or early embryo development *in vitro* versus in vivo: implications for blastocyst yield and blastocyst quality. Molecular Reproduction and Development 61, 234–248. https://doi.org/10.1002/mrd.1153

Rusciano, G., De Canditiis, C., Zito, G., Rubessa, M., Roca, S., Carotenuto, R. et al., 2017. Raman-microscopy investigation of vitrification-induced structural damages in mature bovine oocytes. PLoS ONE 12, 1–19. https://doi.org/10.1371/journal.pone.0177677

Rygula, A., Majzner, K., Marzec, K.M., Kaczor, A., Pilarczyk, M., Baranska, M., 2013. Raman spectroscopy of proteins: a review. Journal of Raman Spectroscopy 44, 1061–1076. https://doi.org/10.1002/jrs.4335

Savitzky, A., Golay, M.J.E., 1964. Smoothing and differentiation of data by simplified least squares procedures. Analytical chemistry 3, 1627–1639. https://doi.org/10.1021/ac60214a047

Sosa Morales, M.C., Alvarez, R.M.S., 2017. Structural characterization of phosphatidylglycerol model membranes containing the antibiotic target lipid II molecule: a Raman microspectroscopy study. Journal of Raman Spectroscopy 48, 170-179. https://doi.org/10.1002/jrs.5033

Wood, B.R., Chernenko, T., Mattha, C., Diem, M., Chong, C., Bernhard, U. et al., 2008. Shedding new light on the molecular architecture of oocytes using a combination of synchrotron Fourier Transform-Infrared and Raman spectroscopic mapping. Analytical Chemistry 80, 9065–9072. https://doi.org/10.1021/ac801 5483

Wu, H., Volponi, J.V., Oliver, A.E., Parikh, A.N., Simmons, B.A., Singh, S., 2011. *In vivo* lipidomics using single-cell Raman spectroscopy. Proceedings of the National Academy of Sciences of the United States of America 108, 3809–3814. https://doi.org/10.1073/pnas.1009043108